Journal of Alloys and Compounds 505 (2010) 722–726

Contents lists available at ScienceDirect

Journal of Alloys and Compounds

journal homepage: www.elsevier.com/locate/jallcom

Annealing effect on the microstructure and microforging of Fe-based stearic nanoflakes

Wooseung Kang*

Department of Metallurgical & Materials Engineering, INHA Technical College, 253 Yonghyun-Dong, Nam-Gu, Incheon 402-752, South Korea

ARTICLE INFO

Article history:
Received 6 May 2010
Received in revised form 16 June 2010
Accepted 20 June 2010
Available online 30 June 2010

Keywords:
Ball milling
Fe-based stearic nanoflakes
Microforging
Heat treatment
Microstructure

ABSTRACT

The microstructural development of Fe-based stearic powders during ball milling and heat treatment was studied in terms of microforging of submicron thick nanoflakes. The crystallite size of the powders was continuously decreased to 55 nm during 60 min ball milling. Dislocation density and microstrain were increased rapidly during plastic deformation. The increasing rate became gradual during fracturing and agglomeration due to the dynamic recovery. The nanoflakes microstructurally recovered from annealing could be microforged further, resulting in a significant enhancement of the conversion rate of the spherical powders into the thin nanoflakes without agglomeration.

1. Introduction

Flake-shaped metallic powders have been much explored due to their unique shape effect. In recent years, flake particles with thicknesses comparable to the skin depths of submicron at high frequencies have attracted much attention with the promising results as a filler media for microwave absorption [1–5].

Flake-shaped powders can be processed with ball milling technique. It is known that ball milling consists of three main processes: microforging, fracturing, and agglomeration. To take advantage of the shape and thin thickness of the individual flake particles, the fracturing and agglomeration during ball milling should be controlled to be as minimal as possible. However, the chaotic nature of ball milling makes it difficult to control each of the main processes applied to the materials. In the previous researches in the area of ball milling, the microstructural evolution and properties were much studied related with the nanocrystalline structure fabrications where the fracturing and agglomeration were playing an important role [6–11].

In this study, the microstructure changes during microforging and annealing of the nanoflakes were investigated in an attempt to process nanoflakes without agglomeration and improve the processing efficiency of the nanoflakes.

2. Experimental procedure

The starting material for this study was spherical iron powders of a maximum size of 7 μm and stearic acid of particulate type. The iron powders of 5 g were charged in a 0.5-l chamber. The balls employed for these experiments were 2 mm stainless steel balls. Ball milling was carried out at room temperature for up to 60 min using a high energy attrition ball mill with the rotation speed of up to 1000 rpm. A ball to powder weight ratio was 100:1.

The morphology changes and thickness of the powders were observed under scanning electron microscope (SEM). The analysis of powder size distributions was conducted using a sieving analysis. The as-processed powders were separated into different size ranges by the Performer III Sieve Shaker by Cole-Parmer. The mesh sizes used were 25, 45, 75 and 106 μm. The collected powders in the sieves were weighed after each processing to obtain the size distributions. X-ray diffraction (XRD) analyses were made using a Rigaku powder diffractometer (DMAX-2500) with Cu Kα (λ_1 = 0.154 nm) radiation to investigate the evolution of microstructure of the powders during ball milling and thermal annealing. The X-ray patterns were analyzed with MDI Jade 5.0 program.

To investigate the microstructure changes of the annealed powders and their effect on the nanoflakes processing, heat treatment was carried out. The samples were annealed for 1 h at the temperature of 100–650 °C in a furnace filled with argon gas after being pumped to 1.3×10^{-3} Pa. All the samples were heated at the same heating rate of 10 °C/min to avoid any heating rate effect on the microstructure.

3. Results and discussion

Assuming volume conservation of the materials during plastic deformation of the spherical powder to flake-shaped particle, the relationship among nanoflake size (d_{nf}), spherical particle size (d_s), and thickness of the nanoflake (t) can be expressed as follows:

$$d_{nf} = 2\sqrt{\frac{d_s^3}{6t}}$$

* Tel.: +82 32 870 2184; fax: +82 32 870 2506.
E-mail address: wkang651@inhatc.ac.kr.

0925-8388/$ – see front matter © 2010 Elsevier B.V. All rights reserved.
doi:10.1016/j.jallcom.2010.06.125

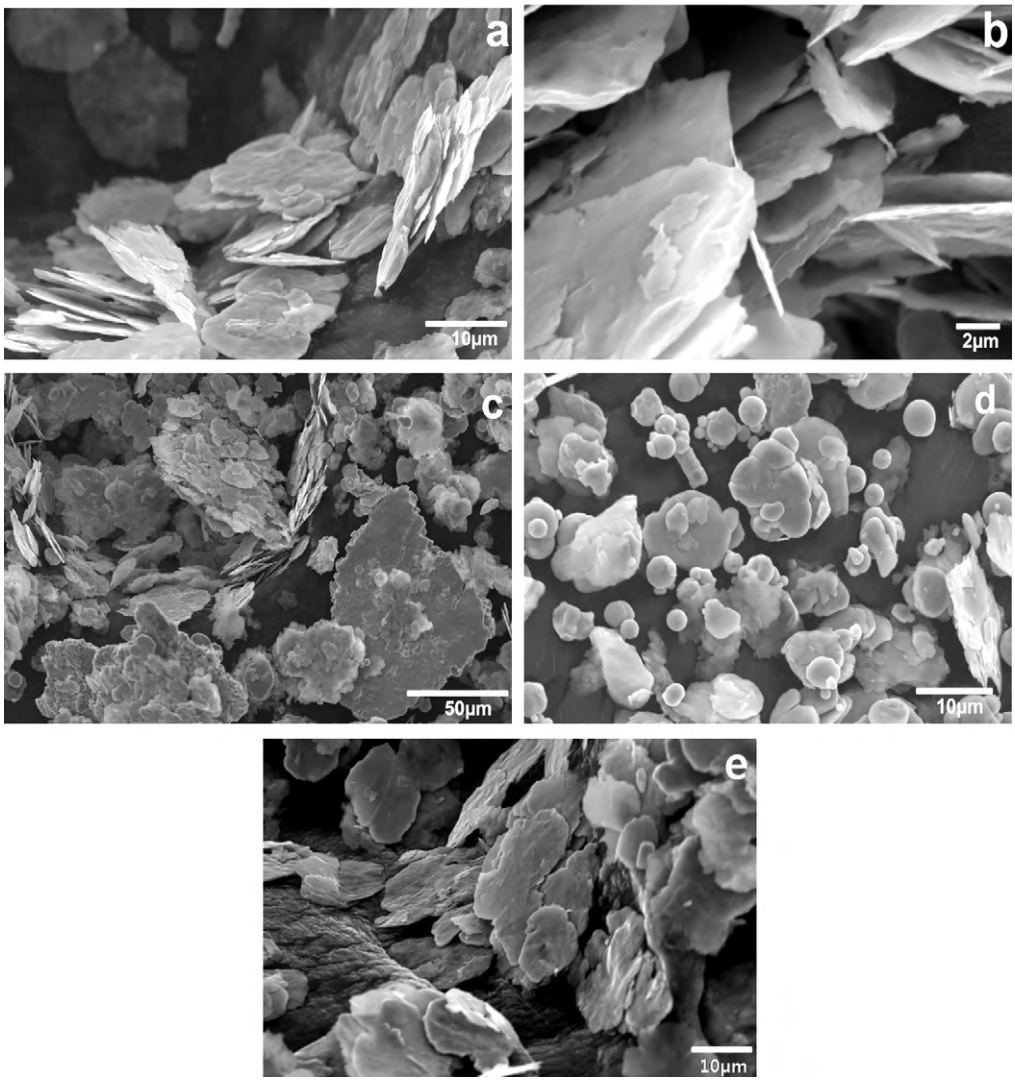

Fig. 1. SEM micrographs: (a) Fe-based stearic nanoflakes microforged 30 min, (b) the submicron thicknesses of the nanoflakes, (c) fractured and cold-welded powders, (d) powders ball milled less than 30 min, not fully deformed to the nanoflakes, and (e) nanoflakes processed with annealing at 350 °C.

Submicron thick flakes microforged from spherical powders of a maximum size of $(d_s)_{max} = 7\,\mu m$ would be in the size range of less than 25 μm if they were not fractured and agglomerated to each other. This assumption was confirmed with the micrographs: Fig. 1(a) and (b) shows the microforged flakes in the less than 25 μm size and their submicron thicknesses, respectively, and Fig. 1(c) shows fractured and agglomerated flakes in the size range of larger than 25 μm, which are also observed when processed without stearic acid.

Along with the SEM observations, size distribution of the powders was also monitored. The weight fractions of the ball milled powders were graphed in Fig. 2(a) as a function of particle size range. During ball milling less than 30 min, most of the powders were within 25 μm size and not fully deformed to the nanoflakes [Fig. 1(d)]. Especially for up to 10 min ball milling, some powders were still not deformed at all by ball milling. After 30 min ball milling, they were converted into nanoflakes [Fig. 1(a)]. But only 58% of the initial powders were converted into the nanoflakes. The other 42% were fractured and agglomerated as seen in Fig. 1(c).

X-ray diffraction patterns of as-received and ball milled powders for up to 60 min is shown in Fig. 3(a). The prominent diffraction peaks correspond to the (1 1 0), (2 0 0) and (2 1 1) planes of α-Fe. The slight shift of the (1 1 0) diffraction peak position with milling time is related with the lattice distortion of α-Fe. The lattice distortion can be characterized with lattice parameter change and microstrain. The relative deviation of the lattice parameter from that of as-received Fe powder, defined as $\Delta a = (a - a_o)/a_o$, is calculated to be as much as $\Delta a = 0.1\%$ for the Fe powders ball milled for up to 60 min. It was reported that the lattice parameter could also be changed due to contamination with milling media during long period of ball milling (e.g., more than 100 h) to obtain nanocrystalline structure [12], which is not the case for the current result.

The width of the peaks broadens and the intensity of the peaks decreases as ball milling time increases. The diffraction peak broadening primarily occurs due to two effects of crystallite size reduction and microstrain increase as described by the following equation [13–15]:

$$w_f = 2\varepsilon \tan\theta_0 + \frac{0.9\lambda}{D\cos\theta_0}$$

where w_f is the full width at the half maximum intensity of Bragg reflection (FWHM), ε the mean lattice microstrain, θ_0 the Bragg

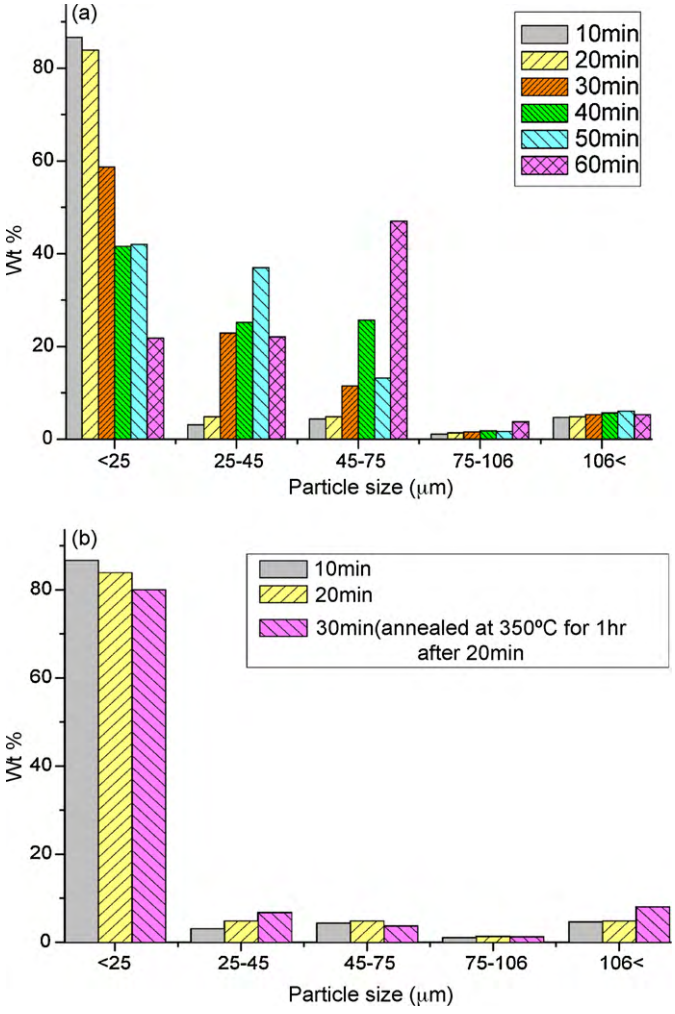

Fig. 2. Particle size distribution with ball milling time: (a) without annealing, spherical powders were deformed to nanoflakes after 30 min milling with the conversion rate of 58%, and (b) with annealing (at 350 °C for 1 h after 20 min milling), resulting in the improved conversion rate of 80%.

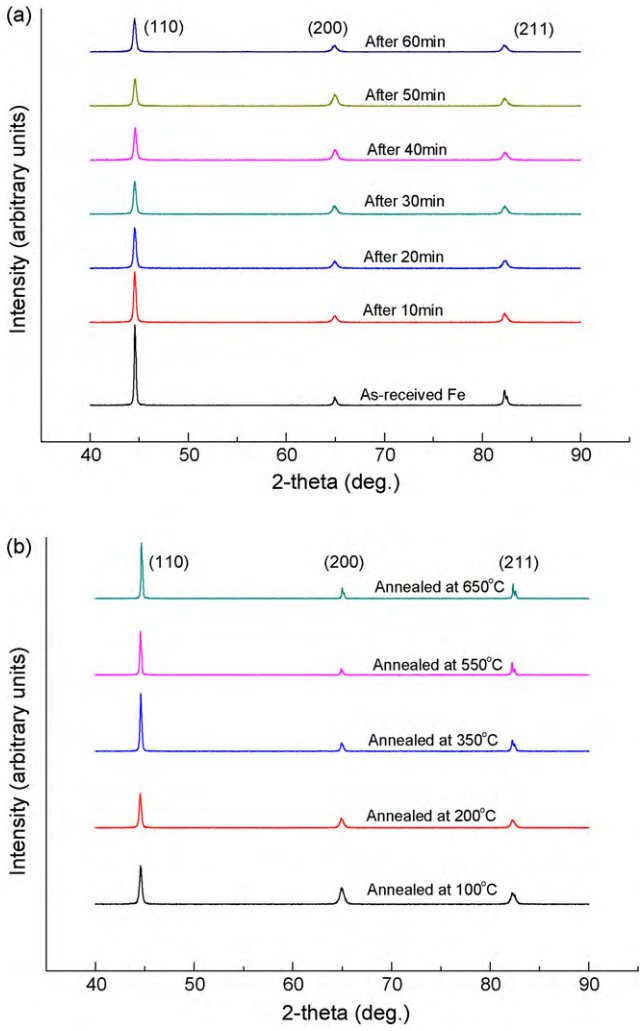

Fig. 3. X-ray diffraction patterns of Fe-based stearic powders (a) with ball milling for up to 60 min, and (b) with annealing at the temperature of 100–650 °C for 1 h after 20 min ball milling.

angle, λ the wavelength of the X-ray radiation, and D the average crystallite size. The mean lattice microstrain ε and the average crystallite size D can be obtained by plotting $w_f \cos\theta_0$ against $\sin\theta_0$. During early short duration of ball milling, relatively much variation in the crystallite size and lattice microstrain among the powder particles is expected due to the presence of particles still not deformed at all. Thus, the data of the powders ball milled up to 10 min which contain the unaffected particles were excluded from the consideration. The average crystallite size decreased with increasing ball milling time to about 55 nm after 60 min of ball milling [Fig. 4(a)]. And the reduction of the crystallite size was accompanied by an increase of mean lattice microstrain. The change rate of crystallite size and microstrain was drastic during the first 20 min ball milling period. And then it was gradually varied. During the initial 20 min ball milling, the powders were mostly subjected to plastic deformation rather than fracturing and agglomeration. Thus, it can be deduced that the microstructure change is more affected by plastic deformation during nanoflakes processing.

Dislocation is a form of stored energy within the Fe powders during ball milling. With the ball milling time, the stored energy, dislocation density in the powders will also continuously increase. And the increased number of dislocation may interact with each other at some point, resulting in the formation of highly immobile dislocations. The region where the immobile dislocations formed is under more stress than the other parts. Thus, cracks can form at the region and spread to eventually fracture the flakes.

Dislocation density ρ can be obtained using the following equation with parameters of crystallite size D, microstrain ε, and Burgers vector b (for Fe, $b = 0.2482$ nm) [16]:

$$\rho = 2\sqrt{3}\frac{\langle\varepsilon\rangle}{Db}$$

The variation of dislocation density with milling time [Fig. 5(a)] was similar to that of microstrain. The dislocation density increased rapidly with the milling time for early 20 min, and then the increasing rate became gradual. The reduction of dislocation density increase rate could be explained with the annihilation and recombination of dislocations during fracturing and agglomeration of the nanoflakes as indicated by the micrograph [Fig. 1(c)] and sieving data [Fig. 2]. In the case of severely deformed ultra-fine grain materials ($d \approx 10^{-6}$–10^{-8} m), the negligible increase in the dislocation density during tensile deformation was also explained by the dynamic recovery due to the fast spreading kinetics of trapped dislocations [17,18].

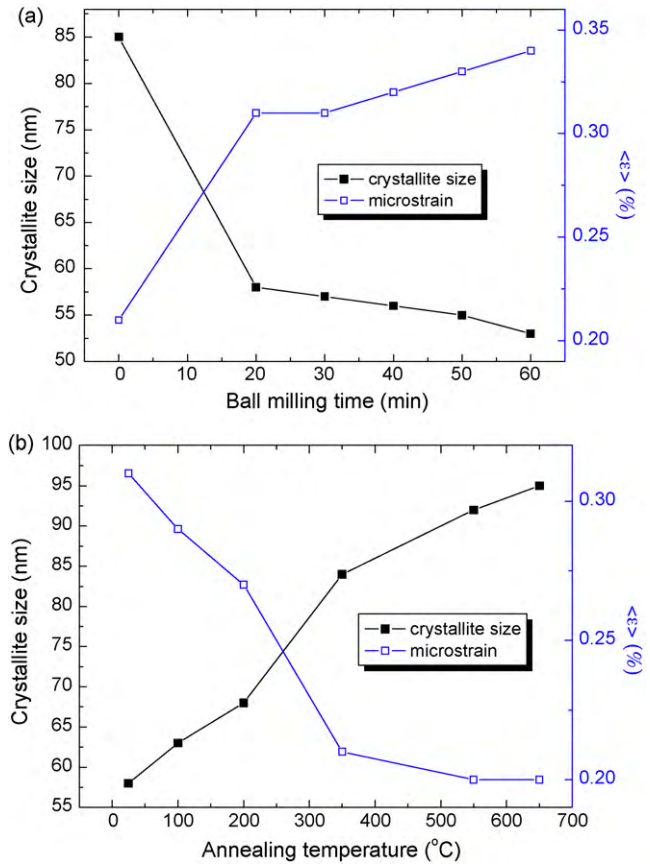

Fig. 4. Changes of average crystallite size and mean microstrain of Fe-based stearic powders as a function of (a) milling time, and (b) annealing temperature.

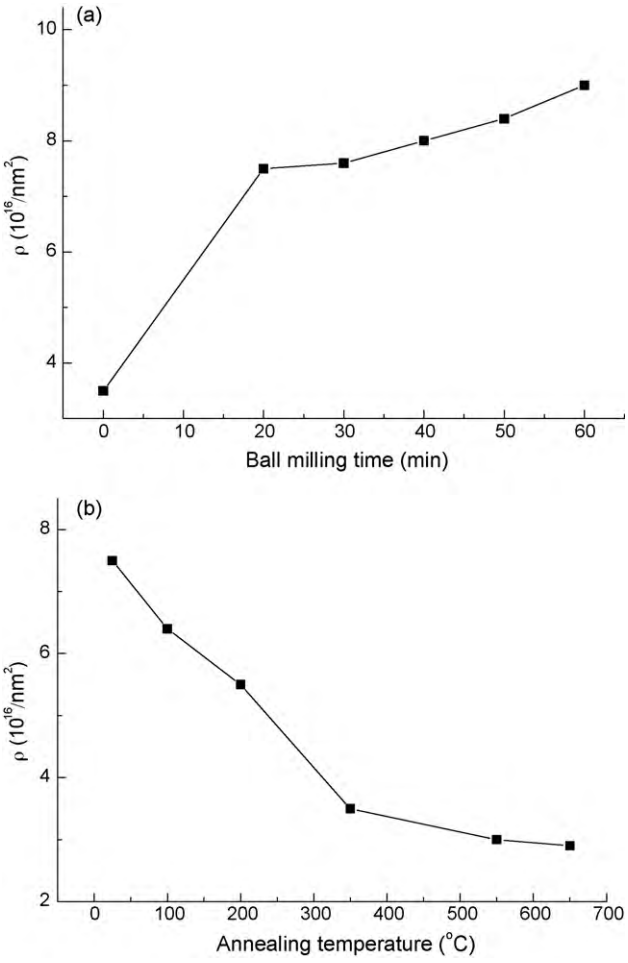

Fig. 5. Change of dislocation density (ρ) of the Fe-based stearic powders as a function of (a) milling time, and (b) annealing temperature.

The severely deformed powders after 20 min ball milling were annealed. Fig. 3(b) shows the X-ray diffraction patterns of the samples annealed at the temperature of 100–650 °C for 1 h after 20 min ball milling. The effect of heat treatment on the microstructure was investigated. And the particle size distribution after additional ball milling with the annealed powders was also measured.

The average crystallite size increased with the increasing annealing temperature while the microstrain showed the opposite behavior [Fig. 4(b)]. It is noted that the microstrain after annealing at 350 °C for 1 h was reduced to the similar level of as-received powders. The microstrain continuously decreased with the increasing temperature, and then nearly leveled off after 550 °C. The continuous decrease of the microstrain even after being reduced to the level of before ball milling indicates that the as-received powders had been pre-strained before ball milling. The dislocation density change with the annealing temperature showed the similar trend with the microstrain [Fig. 5(b)].

After additional 10 min ball milling with the annealed powders at 350 °C, the size distribution and morphology was compared between powders processed with and without annealing during total 30 min ball milling. It is of interest to note that the introduction of annealing significantly improved the conversion rate of the spherical powders into nanoflakes by more than 20%; from 58 to 80% [Fig. 2]. There was no annealing-induced morphology changes observed: the powders processed with the annealing [Fig. 1(e)] showed the similar morphology of the powders milled without annealing [Fig. 1(a) and (b)].

4. Conclusions

Fe-based stearic nanoflakes with the submicron thicknesses were processed by ball milling. The average crystallite size decreased to 55 nm for 60 min ball milling. The mean microstrain and dislocation density increased rapidly for early period of ball milling, plastic deformation dominant period. But the increasing rate became slow during fracturing and agglomeration dominant period due to the dynamic recovery. The mean microstrain and dislocation density continually decreased with the increase of annealing temperature, and returned to the similar levels of the as-received after annealing at 350 °C. The annealed powders showed much extended plastic deformability before fracturing and agglomeration became dominant, resulting in a significant improvement of the conversion rate by more than 20% of the spherical powders into the nanoflakes. And there were no heat treatment-induced morphology changes observed.

Acknowledgements

The author gratefully acknowledges the financial support for this research provided by INHA Technical College under a 2009-Research Grant. He also sincerely acknowledges J. Kang, K. Paek, and H. Paek for their help with heat treatments and XRD measurements.

References

[1] S.I. Kim, M.R. Kim, E.K. Cho, K.Y. Sohn, W.W. Park, Met. Mater. Int. 16 (2010) 121–123.
[2] S.T. Kim, Y.G. Park, S.S. Kim, Met. Mater. Int. 14 (2008) 233–238.
[3] R. Gong, X. Wang, W. Cheng, X. Shen, Mater. Lett. 62 (2008) 266–268.
[4] X. Wang, R. Gong, P. Li, L. Liu, W. Cheng, Mater. Sci. Eng. A466 (2007) 178–182.
[5] F. Wen, W. Zuo, H. Yi, N. Wang, L. Qiao, F. Li, Physica B404 (2009) 3567–3570.
[6] S.S. Nayak, M. Wollgarten, J. Banhart, S.K. Pabi, B.S. Murty, Mater. Sci. Eng. A527 (2010) 2370–2378.
[7] J. Dutkiewicz, L. Lityńska, W. Maziarz, K. Haberko, W. Pyda, A. Kanciruk, Cryst. Res. Technol. 44 (2009) 1163–1169.
[8] Y. Zhang, C. Lu, S. Zhou, J. Joo, J. Nanosci. Nanotechnol. 12 (2009) 7402–7406.
[9] S.K. Pradhan, M. Sinha, J. Appl. Crystallogr. 38 (2005) 951–957.
[10] A. Guittoum, A. Layadi, H. Tafat, N. Souami, J. Magn. Magn. Mater. 322 (2010) 566–571.
[11] M. Sherif El-Eskandarany, A. Amir, H.A. Mahday, A.H. Ahmed, Amer, J. Alloys Compd. 312 (2000) 315–325.
[12] R.J. Perez, B.L. Huang, P.J. Crawford, A.A. Sharif, E.J. Lavernia, Nanostruct. Mater. 7 (1996) 47–56.
[13] A.L. Ortiz, L. Shaw, Acta Mater. 52 (2004) 2185–2197.
[14] G.K. Williamson, W.H. Hall, Acta Metall. 1 (1953) 22–31.
[15] A.R. Stokes, A.C.J. Wilson, Proc. Phys. Soc. Lond. 56 (1944) 174–181.
[16] G.K. Williamson, R.E. Smallman, Philos. Mag. 1 (1956) 34–46.
[17] A.A. Nazarov, A.E. Romanov, R.Z. Valiev, Scr. Mater. 24 (1990) 1929–1934.
[18] W. Lojkowski, Acta Mater. 39 (1991) 1891–1899.